

# Effective band-structure in the insulating phase versus strong dynamical correlations in metallic VO<sub>2</sub>

Jan M. Tomczak,<sup>1</sup> Ferdi Aryasetiawan,<sup>2</sup> and Silke Biermann<sup>1</sup>

<sup>1</sup>*Centre de Physique Théorique, Ecole Polytechnique, CNRS, 91128 Palaiseau Cedex, France*

<sup>2</sup>*Research Institute for Computational Sciences, AIST, Umezono 1-1-1, Tsukuba Central 2, Tsukuba Ibaraki 305-8568, Japan*

Using a general analytical continuation scheme for cluster dynamical mean field calculations, we analyze real-frequency self-energies, momentum-resolved spectral functions, and one-particle excitations of the metallic and insulating phases of VO<sub>2</sub>. While for the former dynamical correlations and lifetime effects prevent a description in terms of quasi-particles, the excitations of the latter allow for an effective band-structure. We construct an orbital-dependent, but static one-particle potential that reproduces the full many-body spectrum. Yet, the ground state is well beyond a static one-particle description. The emerging picture gives a non-trivial answer to the decade-old question of the nature of the insulator, which we characterize as a “many-body Peierls” state.

PACS numbers: 71.27.+a, 71.30.+h, 71.15.Ap

Describing electronic correlations is a challenge for modern condensed matter physics. While weak correlations slightly modify quasi-particle states, by broadening them with lifetime effects and shifting their energies, strong enough correlations can entirely invalidate the band picture by inducing a Mott insulating state.

In a half-filled one-band model, an insulator is realized above a critical ratio of interaction to bandwidth. Though more complex scenarios exist in realistic multi-band cases, a common feature of compounds that undergo a metal-insulator transition (MIT) upon the change of an external parameter, such as temperature or pressure, is that the respective insulator feels stronger correlations than the metal, since it is precisely their enhancement that drives the system insulating.

In this paper we discuss a material where this rule of thumb is inverted : We argue that in VO<sub>2</sub> it is the insulator that is less correlated, in the sense that band-like excitations are better defined and have longer lifetimes than in the metal. Albeit, *neither* phase is well described by standard band-structure techniques. Using an analytical continuation scheme for quantum Monte Carlo solutions to Dynamical Mean Field Theory (DMFT) [1], we discuss quasi-particle lifetimes,  $\mathbf{k}$ -resolved spectra (for comparison with future angle resolved photoemission experiments) and effective band-structures. While dynamical effects are crucial in the metal, the excitations of the insulator are well described within a static picture : For the insulator we devise an effective one-particle potential that captures the interacting excitation spectrum. Still, the corresponding ground state is far from a Slater determinant, leading us to introduce the concept of a “many-body Peierls” insulator.

The MIT of VO<sub>2</sub> has intrigued solid state physicists for decades [2, 3, 4, 5, 6, 7, 8, 9, 10, 11, 12, 13, 14]. A high temperature metallic rutile (R) phase transforms at T<sub>c</sub>=340 K into an insulating monoclinic structure (M1), in which vanadium atoms pair up to form tilted dimers

along the *c*-axis. The resistivity jumps up by two orders of magnitude, yet no local moments form. Despite extensive efforts, the mechanism of the transition is still under debate [6, 7, 8, 9, 10, 11, 12]. Two scenarios compete : In the Peierls picture the structural aspect (unit-cell doubling) causes the MIT, while in the Mott picture local correlations predominate.

VO<sub>2</sub> has a d<sup>1</sup> configuration and the crystal field splits the 3d-manifold into  $\hat{2}g$  and empty  $e_g^\sigma$  components. The former further split into  $e_g^\pi$  and  $a_{1g}$  orbitals, which overlap in R-VO<sub>2</sub>, accounting for the metallic character. Still, the quasi-particle peak seen in photoemission (PES) [9, 10, 11] is much narrower than the Kohn-Sham spectrum of density functional theory (DFT) in the local density approximation (LDA) [7], and eminent satellite features evidenced in PES are absent. In M1-VO<sub>2</sub>, the  $a_{1g}$  form bonding/antibonding orbitals, due to the dimerization. As discussed by Goodenough [3], this also pushes up the  $e_g^\pi$  relative to the  $a_{1g}$ . Yet, the LDA [7] yields a metal. Non-local correlations beyond LDA were shown to be essential [15, 16, 17]. Indeed, recent Cluster DMFT (CDMFT) calculations [15], in which a two-site vanadium dimer constituted the DMFT impurity, opened a gap, agreeing well with PES and x-ray experiments [11, 12].

Starting from these LDA + CDMFT results [15] for the Matsubara  $\hat{2}g$  Green’s function  $G(i\omega_n)$  we deduce the real frequency Green’s function  $G(\omega)$  by the maximum entropy method [18] and a Kramers-Kronig transform. The self-energy matrix  $\Sigma(\omega)$  we obtain by numerical inversion of  $G(\omega) = \sum_{\mathbf{k}} [\omega + \mu - H_{\mathbf{k}} - \Sigma(\omega)]^{-1}$  [1], with the LDA Hamiltonian  $H$ , and the chemical potential  $\mu$ .

Fig. 1 shows (a) the diagonal elements of the R-VO<sub>2</sub> self-energy, and (b) the resulting  $\mathbf{k}$ -resolved spectrum. Notwithstanding minor details, the  $a_{1g}$  and  $e_g^\pi$  self-energies exhibit a similar *dynamical* behavior. The real-parts at zero energy,  $\Re\Sigma(0)$ , entailing relative shifts of quasi-particle bands, are almost equal, congruent with the low changes in their occupations vis-à-vis LDA [15],

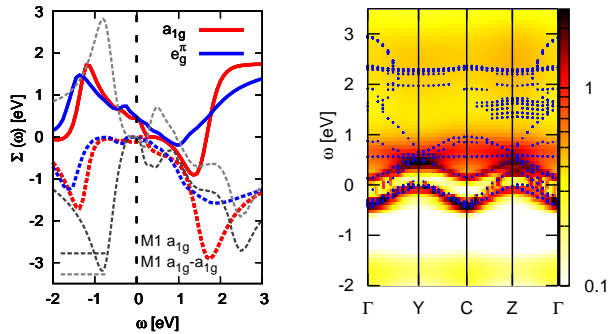


FIG. 1: (color online) Rutile  $\text{VO}_2$ : (a) self-energy ( $\Sigma - \mu$ ). Real (imaginary) parts are solid (dashed). As comparison M1  $\Im\Sigma_{a_{1g}}$ ,  $\Im\Sigma_{a_{1g}-a_{1g}}$  are shown. (b) spectral function  $A(\mathbf{k}, \omega)$  and solutions of the QPE (blue). The LHB is the (yellow) region at  $-1.7$  eV, the broad UHB appears (yellow) at  $\sim 2.5$  eV.

and with the isotropy evidenced in experiment [19].

Neglecting lifetime effects (i.e.  $\Im\Sigma \approx 0$ ), one-particle excitations are given by the poles of  $G(\omega)$ :  $\det[\omega_{\mathbf{k}} + \mu - H_{\mathbf{k}} - \Re\Sigma(\omega_{\mathbf{k}})] = 0$ . We shall refer to this as the quasi-particle equation (QPE) [23]. For static or absent  $\Re\Sigma$  this reduces to a simple eigenvalue problem. In regions of low  $\Im\Sigma$ , the QPE solutions will give an accurate description of the position of spectral weight and constitute an effective band-structure of the interacting system. Yet, due to the frequency dependence, the number of solutions is no longer bounded to the number of orbitals.

Below (above)  $-0.5$  ( $0.2$ ) eV, the imaginary parts of the self-energy – the inverse lifetime – of R- $\text{VO}_2$  is considerable. Due to our limited precision for  $\Im\Sigma(0)$ , we have not attempted a temperature dependent study to assess the experimental bad metal behavior, but the resistivity exceeding the Ioffe-Regel-Mott limit [20] indicates that even close to the Fermi level, coherence is not fully reached. At low energy, the QPE solutions (dots in Fig. 1b) closely follow the spectral weight. Above  $0.2$  eV, regions of high intensity appear, however, the larger  $\Im\Sigma$  broadens the excitations, and no coherent features emerge, though the positions of some  $e_g^\pi$  derived excitations are discernible. At high energies, positive and negative, distinctive features appear in  $\Im\Sigma(\omega)$  that are responsible for lower (upper) Hubbard bands (L/UHB), seen in the spectrum at around  $-1.7$  ( $2.5$ ) eV. The UHB exhibits a pole-structure that reminds of the low-energy quasi-particle band-structure. Hence, an effective band picture is limited to the close vicinity of the Fermi level, and R- $\text{VO}_2$  has to be considered as a strongly correlated metal (the weight of the quasi-particle peak is of the order of  $0.6$ ). This is experimentally corroborated by the fact that an increase in the lattice spacing by Nb-doping results in a Mott insulator of rutile structure [4].

The imaginary parts of the M1  $a_{1g}$  on-site, and  $a_{1g}-a_{1g}$  intra-dimer self-energies, Fig. 1a, are larger than

in R- $\text{VO}_2$ , usually a hallmark of increased correlations. However, we shall argue that correlations are in fact weaker than in the metal. Indeed, the dimerization in M1 leads to strong inter-site fluctuations, evidenced by the significant intra-dimer  $a_{1g}-a_{1g}$  self-energy. Fig. 2 displays the M1- $\text{VO}_2$  self-energy in the  $a_{1g}$  bonding/antibonding (bab) basis,  $\Sigma_{b/ab} = \Sigma_{a_{1g}} \pm \Sigma_{a_{1g}-a_{1g}}$ . The  $a_{1g}$  (anti)bonding imaginary part is low and varies

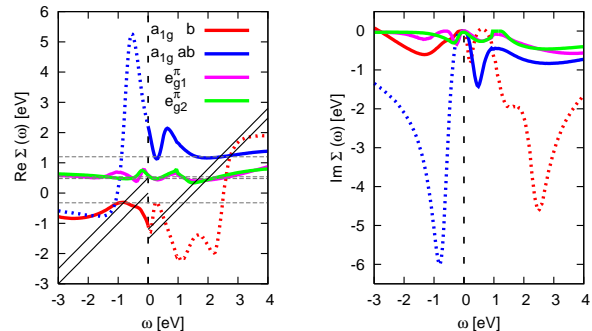


FIG. 2: (color online) Self-energy ( $\Sigma - \mu$ ) of M1- $\text{VO}_2$  in the  $a_{1g}$  bab-basis: (a) real parts. The black stripes delimit the  $a_{1g}$  LDA bandwidths, dashed horizontal lines indicate the values of the static potential  $\Delta$ . (b) imaginary parts. Self-energy elements are dotted in regions irrelevant for the spectrum.

little with frequency in the (un)occupied part of the spectrum, thus allowing for coherent weight. In the opposite regions, the imaginary parts reach huge values. The  $e_g^\pi$  elements are flat, and their imaginary parts tiny. This is a direct consequence of the drastically reduced  $e_g^\pi$  occupancy which drops to merely  $0.14$ . These almost empty orbitals feel only weak correlations, and sharp bands are expected at all energies. A first idea for the  $a_{1g}$  excitations is obtained from the intersections  $\omega + \mu - \epsilon_{b/ab}(\mathbf{k}) = \Re\Sigma_{b/ab}(\omega)$  as depicted in Fig. 2a, where the black stripes delimit the LDA  $a_{1g}$  bandwidths. The (anti)bonding band appears as the crossing of the (blue) red solid line with the stripe at (positive) negative energy. Hence, the (anti)bonding band emerges at  $(2.5) - 0.75$  eV. Still, the antibonding band is much broadened since  $\Im\Sigma_{ab}$  reaches  $-1$  eV. To confirm this, we solved the QPE and calculated the  $\mathbf{k}$ -resolved spectrum (Fig. 3a). As expected, reasonably coherent weight appears over nearly the entire spectrum from  $-1$  to  $+2$  eV, whose position coincides with the QPE poles: The filled bands correspond to the  $a_{1g}$  bonding orbitals, while above the gap, the  $e_g^\pi$  bands give rise to sharp features. The antibonding  $a_{1g}$  is not clearly distinguished since  $e_g^\pi$  weight prevails in this range. The L/UHB have faded: a mere shoulder at  $-1.5$  eV reminds of the LHB. Finally, contrary to R- $\text{VO}_2$ , the number of poles equals the orbital dimension. Since, moreover, the real-parts of the M1- $\text{VO}_2$  self-energy are almost constant for relevant energies [24], we construct a static potential,  $\Delta$ , by evaluat-

ing the dynamical self-energy at the LDA band centers (pole energies) for the  $e_g^\pi$  ( $a_{1g}$ ), see Fig. 2a [25]. Fig. 3b shows the band-structure of  $H_{\mathbf{k}}+\Delta$ : The agreement with the DMFT poles is excellent. Our one-particle potential, albeit static, depends on the orbital, and is thus non-local. We emphasize the conceptual difference to the Kohn-Sham (KS) potential of DFT: The latter generates an effective one-particle problem with the ground state density of the true system. The KS energies and states are *auxiliary* quantities. Our one-particle potential,  $\Delta$ , on the contrary, was designed to reproduce the interacting excitations. The eigenvalues of  $H_{\mathbf{k}}+\Delta$  are thus *not* artificial. Still, like in DFT, the eigenstates are SDs by construction, although the true states are not (see below). The crucial point for M1-VO<sub>2</sub> is that *spectral properties* are capturable with this effective one-particle description. It is in this sense that M1-VO<sub>2</sub> exhibits only weak correlation effects. The weight of the bonding excitation is  $Z=(1-\partial_\omega\Re\Sigma_b(\omega))_{\omega=-0.7\text{eV}}^{-1}\approx 0.75$ , and thus larger than the rutile quasi-particle weight (see above).

What is at the origin of this overall surprising coherence? For the  $e_g^\pi$  orbitals, this simply owes to their depletion. For the nearly half-filled  $a_{1g}$  orbitals the situation is more intricate. It is a joint effect of charge transfer into the  $a_{1g}$  bands, and the bonding/antibonding-splitting. Indeed, the filled bonding band experiences only weak fluctuations, due to its separation of several eV from the antibonding one. To substantiate these qualitative arguments, we resort to the following model, which treats the solid as a collection of Hubbard dimers:

$$H = -t \sum_{l\sigma} \left( c_{l1\sigma}^\dagger c_{l2\sigma} + h.c. \right) - t_\perp \sum_{\substack{i=1,2 \\ \langle l,l' \rangle}} c_{li\sigma}^\dagger c_{l'i\sigma} + U \sum_{il} n_{li\uparrow} n_{li\downarrow} \quad (1)$$

Here,  $c_{li\sigma}^\dagger$  ( $c_{li\sigma}$ ) creates (destroys) an electron with spin  $\sigma$  on site  $i$  of the  $l^{\text{th}}$  dimer.  $t$  is the intra-dimer,  $t_\perp$  the inter-dimer hopping,  $U$  the on-site Coulomb repulsion, and we assume half-filling. First, we discuss

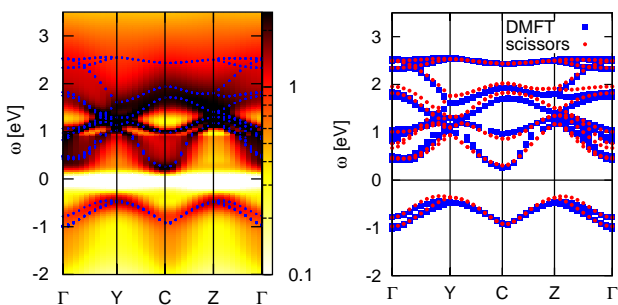


FIG. 3: (color online) M1-VO<sub>2</sub>: (a) spectral function  $A(\mathbf{k},\omega)$ . (blue) dots ((a) & (b)) are solutions of the QPE. (b) The (red) dots are the eigenvalues of  $H_{\mathbf{k}}+\Delta$ . See text for discussion.

the  $t_\perp \rightarrow 0$  limit, which is an isolated dimer: the Hubbard molecule. We choose  $t=0.7$  eV, the LDA intra-dimer  $a_{1g}$ - $a_{1g}$  hopping, and  $U=4.0$  eV [15] for all evaluations. The bonding/antibonding-splitting,  $\Delta_{bab}=-2t+\sqrt{16t^2+U^2}=3.48$  eV, gets *enhanced* with respect to the  $U=0$  case. In M1-VO<sub>2</sub>, the embedding into the solid, and the hybridization with the  $e_g^\pi$  reduce the splitting to  $\sim 3$  eV, as can be inferred from the one-particle poles (Fig. 3), consistent with experiment [11]. The ground state of the dimer is given by  $|\psi_0\rangle = \{4t/(c-U)(|\downarrow\uparrow\rangle - |\uparrow\downarrow\rangle) + (|\uparrow\downarrow 0\rangle + |0\uparrow\downarrow\rangle)\}/a$  [26] which is intermediate to the Slater determinant (SD) (the four states having equal weight), and the Heitler-London (HL) limit (double occupancies projected out). With the VO<sub>2</sub> parameters, the model dimer is close to the HL limit [5]. The inset of Fig. 4b shows the projections of the ground state onto the SD and the HL state. The former,  $|\langle SD|\psi_0\rangle|^2$ , equals the weight of the band-derived features in the spectrum (for  $U>0$  satellites appear), while the other measures the double occupancy  $\sum_i \langle n_{i\uparrow} n_{i\downarrow} \rangle = 1 - |\langle HL|\psi_0\rangle|^2$ . For  $U=4.0$  eV the latter is largely suppressed, as a consequence of the interaction: The N-particle state is clearly not a SD. Still, the overlap with the SD, and thus the coherent weight, remains significant, i.e. one-particle excitations survive and lifetimes are large. To do justice to the seemingly opposing tendencies of correlation driven non-SD-behavior, coexisting with a band-like spectrum, we introduce the notion of a “many-body Peierls” state.

The charge transfer from the  $e_g^\pi$  into the then almost half-filled  $a_{1g}$  orbitals, finds its origin in the effective reduction of the local interaction in the bab-configuration: While for  $U=4$  eV,  $\langle SD|H|SD\rangle = 2.0$  eV in the SD limit, it reduces to merely  $\langle \psi_0|H|\psi_0\rangle = 0.91$  eV in the ground state. In fact, inter-site fluctuations are an efficient way to avoid the on-site Coulomb repulsion. In M1-VO<sub>2</sub>, this effect manifests itself in a close cancellation of the local and inter-site self-energies in the (un-)occupied parts of the spectrum for the (anti)bonding  $a_{1g}$  orbitals.

The gap-opening in VO<sub>2</sub> thus owes to two effects: The self-energy enhancement of the  $a_{1g}$  bab-splitting, and a charge transfer from the  $e_g^\pi$  orbitals. The difference in  $\Re\Sigma$  corresponds to this depopulation, seen in experiments [19] and theoretical studies [8, 15], and leads to the separation of the  $a_{1g}$  and  $e_g^\pi$  at the Fermi level. *The local interactions thus amplify Goodenough’s scenario.*

To show that the embedding of the dimer into the solid does not qualitatively alter our picture of the M1 phase, we solve the model, Eq. (1), using CDMFT. This moreover allows to study the essentials of the rutile to M1 MIT by scanning through the degree of dimerization  $t$  at constant interaction strength  $U$  and embedding, or inter-dimer hopping,  $t_\perp$ . For the latter we assume a semi-circular density of states  $D_\perp(\omega)$  of bandwidth  $W=4t_\perp$ . In M1-VO<sub>2</sub>, the  $t_\perp$  for direct  $a_{1g}$ - $a_{1g}$  hopping is rather small, yet  $e_g^\pi$ -hybridizations lead to an effective

$D_{\perp}$ -bandwidth of about 1 eV. We choose  $U=4t_{\perp}$ , and an inverse temperature  $\beta=10/t_{\perp}$ . Fig. 4a displays the orbital traced local spectral function  $A(\omega)=A_b(\omega)+A_{ab}(\omega)$  (b,ab denoting again the bonding/antibonding combinations) and the bonding self-energy  $\Sigma_b(\omega)$  for different intra-dimer hoppings  $t$ : In the absence of  $t$ , the result equals by construction the single site DMFT solution ( $\Sigma_b=\Sigma_{ab}$ ), which, for our parameters, is a correlated metal, analog to R-VO<sub>2</sub>. The spectral weight at the Fermi level is given by  $A_{b/ab}(0) = D_{\perp}(\pm t - \Re\Sigma_{b/ab}(0))$ , with  $\Re\Sigma_{b/ab}(0)=\mp\Re\Sigma_{ab}(0)$ . Thus a MIT occurs at  $t + \Re\Sigma_{ab}(0) = 2t_{\perp}$ , when all spectral weight has been shifted out of the bandwidth: Above  $t/t_{\perp}=0.5$  we find a many-body Peierls phase corresponding to M1-VO<sub>2</sub>. In Fig. 4a we have indicated again the graphical QPE approach: The system evolves from three solutions *per orbital* (Kondo resonance, L/UHB) at  $t=0$  to a single one at  $t/t_{\perp}=0.6$ . Hence the peaks in the insulator are *not* Hubbard satellites, but just shifted bands. The embedding,  $t_{\perp}$ , broadens the excitations and washes out the satellites of the isolated dimer, like for M1-VO<sub>2</sub>. Still, as a function of  $t$ , the coherence of the spectrum increases, since the imaginary part of the (anti-)bonding self-energy subsides at the renormalized (anti-)bonding excitation energies. Our model thus captures the essence of the rutile to M1 transition, reproducing both, the dimerization induced increase in coherence, and the shifting of excitations.

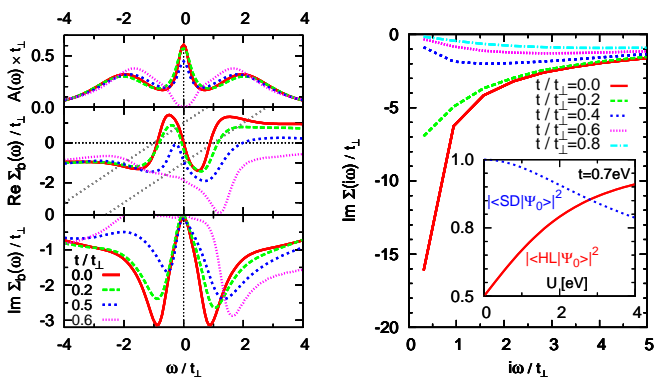


FIG. 4: (color online) (a) spectral function (top), real (middle), imaginary (bottom) *bonding* self-energy  $\Sigma_b$  of the CDMFT solution to Eq. (1) for  $U=4.0t_{\perp}$ ,  $\beta=10/t_{\perp}$ , and varying intra-dimer hopping  $t/t_{\perp}$ .  $\Re\Sigma_b(\omega)=-\Re\Sigma_{ab}(-\omega)$ ,  $\Im\Sigma_b(\omega)=\Im\Sigma_{ab}(-\omega)$  by symmetry. (b) Imaginary Matsubara self-energy,  $\Im\Sigma_b(i\omega)=\Im\Sigma_{ab}(i\omega)$ , for  $U=6t_{\perp}$ ,  $\beta=10/t_{\perp}$  and varying  $t$ . Inset: Projection of the SD and HL limit on the Hubbard molecule ground state ( $t=0.7$  eV,  $t_{\perp}=0$ ) versus  $U$ .

Under uni-axial pressure or Cr-doping, VO<sub>2</sub> develops the insulating M2 phase [4] in which every second vanadium chain along the c-axis consists of untilted dimers, whereas in the others only the tilting occurs. We may now speculate that the dimerized pairs in M2 form  $a_{1g}$

Peierls singlets as in M1, while the tilted pairs are in a Mott state. Hence, we interpret the seminal work of [4] as the observation of a Mott to many-body Peierls transition taking place on the tilted chains when going from M2 to M1. To illustrate this, we solve again Eq. (1) for appropriate parameters. The tilted M2 chains are akin to the rutile phase, yet with a reduced  $a_{1g}$  bandwidth [7]. Thus we now choose  $U=6t_{\perp}$ ,  $\beta=10/t_{\perp}$ , and vary  $t$ . All solutions shown in Fig. 4b are insulating, however, the diverging self-energy at vanishing intra-dimer coupling ( $t=0$ , tilted “M2” chains) becomes regularized with the bond enhancement ( $t>0$ , “M1”). The imaginary part of the self-energy gets flatter and the system thus more coherent. The above is consistent with the finding of (S=0) S=1/2 for the (dimerized) tilted pairs in M2-VO<sub>2</sub> [4].

While our results do not exclude surprises in the direct vicinity of  $T_c$  [22], the nature of insulating VO<sub>2</sub> is shown to be rather “band-like” in the above sense. Our analytical continuation scheme allowed us to *explicitly calculate* this band-structure. The latter can also be derived from a static one-particle potential. Yet, this does *not* imply a one-particle picture for quantities other than the spectrum. Above all, the ground state is not a Slater determinant. Hence, we qualify M1-VO<sub>2</sub> as a “many-body Peierls” phase. We argue that the weakness of lifetime effects results from strong inter-site fluctuations that circumvent local interactions in an otherwise strongly correlated solid. This is in striking contrast to the strong dynamical correlations in the metal, which is dominated by important lifetime effects and incoherent features.

We thank H. T. Kim, J. P. Pouget, M. M. Qazilbash, and A. Tanaka for valuable discussions and A. I. Poteryaev, A. Georges and A. I. Lichtenstein for discussions and the collaboration [15] that was our starting point. We thank AIST, Tsukuba, for hospitality. JMT was supported by a JSPS fellowship. Computer time was provided by IDRIS, Orsay (project No. 071393).

- [1] J. M. Tomczak and S. Biermann, J. Phys.: Condens. Matter (2007), in press.
- [2] A. Zylbersztein, N. F. Mott, Phys. Rev. B **11**, 4383 (1975).
- [3] J. B. Goodenough, J. Solid State Chem. **3**, 490 (1971).
- [4] J. P. Pouget, H. Launois, J.Phys. France **37**, C4 (1976).
- [5] C. Sommers, S. Doniach, Solid State Commun. **28**, 133 (1978).
- [6] R. M. Wentzcovitch et al., Phys. Rev. Lett. **72**, 3389 (1994).
- [7] V. Eyert, Ann. Phys. (Leipzig) **11**, 650 (2002).
- [8] A. Tanaka, J. Phys. Soc. Jpn. **72**, 2433 (2003).
- [9] R. Eguchi et al., cond-mat/0607712 (2006).
- [10] S. Shin *et al.*, Phys. Rev. B **41**, 4993 (1990).
- [11] T. C. Koethe et al., Phys. Rev. Lett. **97**, 116402 (2006).
- [12] G. A. Sawatzky, D. Post, Phys. Rev. B **20**, 1546 (1979).
- [13] A. Continenza et al., Phys. Rev. B **60**, 15699 (1999).

- [14] M. A. Korotin *et al.*, Phys. Met. Metallogr. **94**, 17 (2002).
- [15] S. Biermann *et al.*, Phys. Rev. Lett. **94**, 026404 (2005).
- [16] A. Liebsch *et al.*, Phys. Rev. B **71**, 085109 (2005).
- [17] M. S. Laad *et al.*, Phys. Rev. B **73**, 195120 (2006).
- [18] M. Jarrell, J. E. Gubernatis, Phys. Rep. **269**, 133 (1996).
- [19] M. Haverkort *et al.*, Phys. Rev. Lett. **95**, 196404 (2005).
- [20] M. M. Qazilbash *et al.*, Phys. Rev. B **74**, 205118 (2006).
- [21] A. Georges *et al.*, Rev. Mod. Phys. **68**, 13 (1996).
- [22] H.-T. Kim *et al.*, Phys. Rev. Lett. **97**, 266401 (2006).
- [23] We solve the equation numerically by iterating until self-consistency within an accuracy of 0.05 eV.
- [24] Explaining why LDA+U opens a gap [14, 16], yet while missing the correct bonding/antibonding splitting.
- [25]  $\Delta_{e_g^{\uparrow 1}}=0.48\text{eV}$ ,  $\Delta_{e_g^{\uparrow 2}}=0.54\text{eV}$ ,  $\Delta_b=-0.32\text{eV}$ ,  $\Delta_{ab}=1.2\text{eV}$
- [26]  $a = \sqrt{2(16t^2/(c-U)^2 + 1)}$ ,  $c = \sqrt{16t^2 + U^2}$